مجلة الدراسات التربوية والعلمية - كلية التربية - الجامعة العراقية
العدد السابع والعشرون - المجلد الثالث - علوم الحياة - آذار 2026 م
doi.org/10.52866/esj.2026.03.27.09

Antimicrobial Activity of Photosynthesized Zinc Oxide Nanoparticles using Aas (*Myrtus communis* L.) Leaves Extract

Omar I. Khalif *   Esam J. Alkalifawi**
Department of Biology, College of Education for pure science Ibn al-Haytham, University of Baghdad
*Omar.Alwan2202m@ihcoedu.uobaghdad.edu.iq   **aesam365@Yahoo.com

Abstract :

In this current study, zinc oxide nanoparticles have been photosynthesized and characterized using Aas leaf extract. UV–Vis and Fourier-transform infrared spectroscopy (FT-IR) tests confirmed the existence of biomolecules, active materials, and zinc oxides. The photosynthesis zinc oxide nanoparticles have been scanned by Field Emission Scanning Electron Microscope. It reveals that zinc oxide nanoparticles appeared to be irregular and polymorphic and the crystalline forms of these particles varied between rectangular, spherical, radial and cylindrical structures and the average size ranges between 21-43nm. The X-ray diffraction spectrum of photosynthesized zinc oxide nanoparticles corresponding to the main peaks obtained at 100, 002, 101, 102, 110, 103, 112, 201 and 004 correspond to reflections with 2θ values of the Bragg angles 32.19°, 34.84°, 36.67°, 47.94°, 56.98°, 63.24°, 66.74°, 69.45° and 72.92° respectively. These results confirm that the material tested where zinc oxide nanoparticles and are of high purity. The average size of zinc oxide nanoparticles was extracted using the Dubai-sheerer equation and the average particle size was 39.2 nm. The size of ZnONPs was observed from tip-corrected AFM measurements and the shape of ZnONPs was determined. The tip-corrected measured the size of ZnONPs in the range of 43 nm. The result showed the 3D view of the sample surface and height distribution around 38.9 nm.

The Antimicrobial Activity of MC-ZnONPs on Twenty MDR *Acinetobacter baumannii* Isolates by Resazurin-based 96-well plate microdilution method showed that the minimum inhibitory concentration (MIC) of MC-ZnONPs was 156.25 µg/ml for A. baumannii isolates number 2,3,4,5,6,7,8,9,10,16,17,18 and 20) while the MIC was 78.125µg/ml for A. baumannii isolates number 1,11,12,13,14,15 and 19).

It has been concluded that the possibility of using leaves extract of the Aas to prepare MC-ZnONPs, because its rich content of active compounds have the ability to act as reducing, capping and stabilizing agent. MC-ZnONPs are characterized by their antimicrobial properties.

Keywords: *Myrtus communis* L, Photosynthesis, ZnONPs, Charactrization, Antimicrobial Activity .

النشاط المضاد للميكروبات لجسيمات أوكسيد الزنك النانوية المحضّرة نباتياً باستخدام مستخلص أوراق نبات الآس (*Myrtus communis L.*)

عمر اسماعيل خليف   ،   عصام جاسم الخليفاوي
جامعة بغداد / كلية التربية للعلوم الصرفة - ابن الهيثم، قسم علوم الحياة

مستخلص:

في هذه الدراسة، تم تحضير جسيمات أوكسيد الزنك النانوية نباتياً وتوصيفها باستخدام مستخلص أوراق نبات الآس (*Myrtus communis L.*). وقد أكدت اختبارات الأشعة فوق البنفسجية – المرئية (UV-Vis) ومطيافية الأشعة تحت الحمراء (FT-IR) وجود جزيئات حيوية ومواد فعالة وأكاسيد الزنك. فُحصت جسيمات أوكسيد الزنك النانوية المحضرة نباتياً بواسطة المجهر الالكتروني الماسح عالي الكفاءة FESEM. وتبين أن جسيمات أكسيد الزنك النانوية تبدو غير منتظمة ومتعددة الأشكال، وأن الأشكال البلورية لهذه الجسيمات تراوحت بين هياكل مستطيلة وكروية وشعاعية وأسطوانية، ويتراوح متوسط حجمها بين 21 –43 نانومترًا. طابق طيف حيود الأشعة السينية لجسيمات أكسيد الزنك النانوية المحضرة للقمم الرئيسية المُحصّلة عند 100، 002، 101، 102، 110، 103، 112، 201، و004، ويتوافق مع الانعكاسات قيم 2θ لزوايا براغ 32.19 درجة، 34.84 درجة، 36.67 درجة، 47.94 درجة، 56.98 درجة، 63.24 درجة، 66.74 درجة، 69.45 درجة، و72.92 درجة على التوالي. تؤكد هذه النتائج أن المادة المُختَبَرة تحتوي على جسيمات أكسيد الزنك النانوية، وهي عالية النقاوة. استُخرج متوسط حجم جسيمات أكسيد الزنك النانوية باستخدام معادلة دبي–شيرر، وكان متوسط حجم الجسيم 39.2 نانومتر. لوحظ حجم ZnONPs من قياسات مجهر القوة الذرية (AFM)، وحُدد شكلها. وُجد أن حجم ZnONPs في نطاق 43 نانومتر. وأظهرت النتيجة صورة ثلاثية الأبعاد لسطح العينة وتوزيع الارتفاع حوالي 38.9 نانومتر.

أظهرت دراسة النشاط المضاد للميكروبات لـ MC-ZnONPs على 20 عزلة ذات مقاومة متعددة للمضادات الحياتية من بكتيريا *Acinetobacter baumannii* باستخدام طريقة التخفيف المتسلسل في صفيحة ذات 96 حفرة باستخدام صبغة الريزازورين أن التركيز المثبط الادنى لـ MC-ZnONPs كان 156.25 ميكروغرام/ مل لعزلات *A. baumannii* رقم (2، 3، 9،8،7،6،5،4، 10، 16، 18،17، 20)، بينما كان التركيز المثبط الادنى 78.125 ميكروغرام/ مل لعزلات *A. baumannii* رقم (1، 11، 12، 13، 14، 15، 19).

تم التوصل إلى إمكانية استخدام مستخلص أوراق نبات الآس في تحضير MC-ZnONPs، لكونهُ غنياً بالمركبات الفعالة التي لها القابلية على العمل كعامل اختزال وتغطية وتثبيت. تتميز MC-ZnONPs بخصائصها المضادة للميكروبات.

الكلمات المفتاحية: الآس، البناء الاخضر، جسيمات الزنك النانوية، توصيف، الفعالية الميكروبية.

1. Introduction

The remarkable growth of nanotechnology drives the development of new materials with diverse physicochemical and biological properties. Among the most studied are zinc oxide nanoparticles (ZnONPs) [1,2]. The ZnONPs possess excellent optical, electronic, and antimicrobial properties, making them useful in various fields such as biomedicine, environmental cleanup, and electronics. However, traditional methods for synthesizing ZnONPs involve hazardous chemicals and energy-intensive processes, rising environmental and biocompatibility concerns [3,4].

To address these issues, researchers have explored green synthesis methods, especially those using plant extracts as reducing and stabilizing agents [5]. Aas extract has become prominent in the ecofriendly production of ZnONPs, marking a significant advancement in sustainable nanotechnology [6].

This Mediterranean herb is rich in phytochemicals, such as terpenes, flavonoids, and phenolic acids [7,8]. These bioactive compounds naturally act as reducing and stabilizing agents, converting metal ions into nanoparticles and maintaining their stability during synthesis [9]. The functional groups in Aas (*Myrtus communis* L.) facilitate efficient nucleation and growth of ZnONPs without relying on harmful chemicals. This approach aligns with green chemistry principles by reducing environmental harm through limiting toxic reagents and waste. The plant based extract also improves nanoparticle compatibility for biomedical and pharmaceutical applications [10,11]. Furthermore, Aas is readily available and inexpensive, contributing to the economic viability of the synthesis process. The bioactivity of the phytochemicals may also impart antibacterial and antioxidant properties to the ZnONPs, enhancing their functional potential. Compared to conventional physical and chemical methods of nanoparticle production, green synthesis with Aas leaf extract offers clear advantages [12]. Traditional approaches often require strong reducing agents, stabilizers, or surfactants that pose environmental and health risks, whereas Aas leaf extract provides a natural and non-toxic alternative. The process tends to be simpler, with milder reaction conditions and less need for specialized equipment. The phytochemicals in Aas also improve the colloidal stability of the nanoparticles, as indicated by favorable zeta potential (ZP) measurements. Additionally, green methods consume less energy due to lower operating temperatures and pressures. The significance of Aas mediated green synthesis of ZnONPs lies in overcoming the limitations of conventional methods and enabling new biological functionalities. These nanoparticles leverage zinc oxide's inherent properties along with Aas derived bioactive compounds, showing promise for many applications, especially in antimicrobial and biomedical fields. Overall, green synthesis using Aas leaf extract promotes a sustainable, efficient, and versatile pathway for producing ZnONPs, supporting the global goal of environmentally responsible scientific innovation [13]. Much is happening regarding the plant mediated synthesis of metal oxide nanoparticles, but aspects of all these methods are still not well understood [14]. For instance, the understanding of how the phytochemicals work on the nanoparticle nucleation, the organism, growth, or stabilization is not thorough [15]. Furthermore, the physicochemical characteristics of green synthesized ZnONPs may not have a profound or direct correlation with their biological activity, particularly their antibacterial properties.

Acinetobacter baumannii is considered one of the bacterial pathogens that poses a growing threat to healthcare systems worldwide. It is classified as an opportunistic pathogen that causes a wide range of infections, particularly among immunocompromised patients, especially those admitted to intensive care units (ICUs). These infections represent a major challenge for physicians due to the difficulty of treating them with conventional antibiotics, mainly after the emergence of multidrug-resistant (MDR) and even extensively drug-resistant (XDR) isolate [16,17].

The present study summarizes photosynthesized zinc oxide nanoparticles using Aas leaves extract, studying their characterization and antimicrobial activity.

2. Materials and Methods

2.1 Materials

The Plant samples of Aas leaves were collected from home gardens and nurseries in Baghdad, Iraq, specifically from the Al-Saydiya and Al-Jadriya areas, during April 2024, ensuring that the leaves were healthy and free from defects and plant diseases.

The identity of the plant was confirmed by Taxonomist Dr. Areej Al-ani, Department of Biology, College of Education for pure science Ibnal-Haytham, University of Baghdad. $ZnCl_2$ (99.8%) and other solvents utilized in this study were procured from Sigma Aldrich, St. Louis, MO, USA.

2.2 Preparation of Plant Extract

The aqueous extract of Aas leaves was prepared according to the method of [18]. with some modifications. Fresh, healthy leaves were thoroughly washed under running water and soaked for 30 minutes to remove surface contaminants. The leaves were then air-dried to remove moisture and cut into small pieces using a sterilized scissor in sterile condition. Subsequently, 20 g of the leaves were weighed and placed in a 250 ml glass flask containing 200 ml of distilled water (ratio 10:1). The mixture was blended using a laboratory mixer (120 W). The extract was filtered through Whatman filter paper, and the clear filtrate was centrifuged at 5000 rpm for 10 minutes to remove debris and residues. Finally, the purified extract was stored in dark bottles at 4 °C until use.

2.3 Synthesis and Characterization of Zinc Oxide Nanoparticles using Aas leaves Extract

Zinc nanoparticles were synthesized using the aqueous extract of Aas leaves according to the method of [19]. with some modifications. 10 g of zinc chloride $ZnCl_2$ was added to 100 ml of the aqueous extract of Aas leaves, and the mixture was agitated on a shaker at room temperature for 24 hours. The biosynthesis of ZnO nanoparticles was indicated by the color change of the mixture from light yellow to dark brown.

The ZnO nanoparticles were purified by heat- and break-resistant laboratory tubes were used, and was distributed into them and centrifuged at 10,000 rpm for 10 minutes. The supernatant was carefully discarded while preserving the pellet, which was then washed with absolute ethanol and centrifuged again at 10,000 rpm for 10 minutes [20]. The pellet was subsequently collected in sterile glass dishes, spread evenly, and dried in an electric oven at 80 °C to remove residual ethanol. After drying, the pellet was finely ground using a ceramic mortar to obtain a smooth powder, and the purified ZnO nanoparticles were stored in Eppendorf tubes until further use [21].

Characterization of Zinc Oxide nanoparticles

1. UV-Vis Spectra analysis

The UV-Vis spectrum analysis was achieved within the range of 190 to 1100 nm using a UV-visible spectrophotometer (Shimadzu UV-1800). This test was performed 24 hours after the preparation and drying of the dough in the central laboratory of the Chemistry Department / College of Science / University of Baghdad.

2. Fourier Transform Infra-Red Spectroscopy (FT-IR)

The FTIR analysis was introduced to investigate the chemical bonding between the atoms of the prepared materials nanoparticle. This particular technique was performed using the Shimadzu-IR Affinity-I spectrophotometer. In this procedure, the samples under test are homogenized with KBr and then the FTIR spectrum was recorded within the range of 4000 to 400 cm^{-1}. Before the recording procedure, potassium bromide (AR-grade) was dried and mixed with KBr (100mg) as well as Zinc chloride (1 mg). Note that the KBr pellet was obtained under vacuum with the temperature of 100°C for a period of 48hrs.

3. X-Ray Diffraction (XRD) analysis

Resulting solution of the developed nanoparticles of Zinc Oxide was centrifuged at 10,000 rpm for 30 min. The solid residues of ZnONPs were washed twice with deionized distilled water and then dried at 80ºC to obtain powder ZnONPs used for X-ray powder diffraction measurements. The powder of nanoparticles was measured by XRD. XRD patterns were recorded on (Shimadzu XRD-6000/Japan) with copper radiation (Cu Kα, 1.5406 Å) at 40 kV and 30 Ma [22].

4. Field emission scanning electron microscopy (FE-SEM) analysis

The images were taken with a Field emission scanning electron microscope (FE-SEM) (Hitachi Ltd. /Japan) with a resolution of 500 nm (Hitachi s-3400N) and detectors containing a secondary electron; BSE semiconductors (quad-type) were used to study the size and shape of ZnO nanoparticles, this approach is used to obtain detailed information about surface ZnONPs. FE-SEM was used to characterize the average particle morphology and diameter of the ZnONPs. After using distilled water to sonicate the dried nanoparticles solution sample, a tiny drop of the sample was put on a microscope slide and left to dry. The samples were then coated with a thin layer of platinum to make them conductive.

5. Energy Dispersive X-ray (EDX)

X-ray energy diffraction spectroscopy was used to investigate and determine the elemental compositions of the ZnO nanoparticles. For this purpose, after preparing the samples, using an EDX detector on field emission scanning electron microscope, the spectra of the constituent elements of the samples were prepared.

6. Atomic Force Microscope (AFM)

This technique aimed to investigate the surface morphology of the prepared ZnONPs using Inc. SPM-AA300 (U.S.) with AFM communication mode. In particular, 5 drops of nanoparticles solution were dropped on a specific laboratory slide and kept for 30 min at 110° C in an oven. Continuously, the 3D morphology /topography of the sample under the test surface were screened via the interaction of the probe force on the sample surface. This procedure is attained through a raster scan of the tested material, taking into consideration the distance and the force between the tip and the sample, two parameters that should be considered carefully [23]. The AFM was introduced to investigate the Se nanoparticles' surface features using a 2D and 3D imaging approach.

Isolation and identification of *Acinetobacter baumannii*

All tests used [24], including morphological characteristics on different culture media, Gram staining, motility, biochemical tests, and finally confirmed using the VITEK® 2 compact system ID-GNB cards, revealed that the isolates were *Acinetobacter baumannii*.

Resazurin Microplate Assay (REMA)

REMA was used for determination of (MIC) of MC-ZnONPs, the MIC determined through recording of the color change observed [25].

3. Results

The prepared ZnONPs were characterized by various spectroscopic and microscopic methods to evaluate their elemental composition, exact morphology and also other physicochemical properties. The color change of the reaction mixture from light yellow to dark brown, confirms the synthesis of MC-ZnONPs figure 1.

Figure 1. The change in the color of Photosynthesized Zinc Oxide Nanoparticles using Aas leaves extract, A, Zinc chloride solution. B, Aas Leaf Extract. C. Photosynthesized ZnO Nanoparticles colloidal.

The UV-Visible spectroscopy analysis revealed the absorption maximum (λmax) at 361 nm was attributed to the surface Plasmon resonance (SPR) of MC- ZnONPs figure 2.

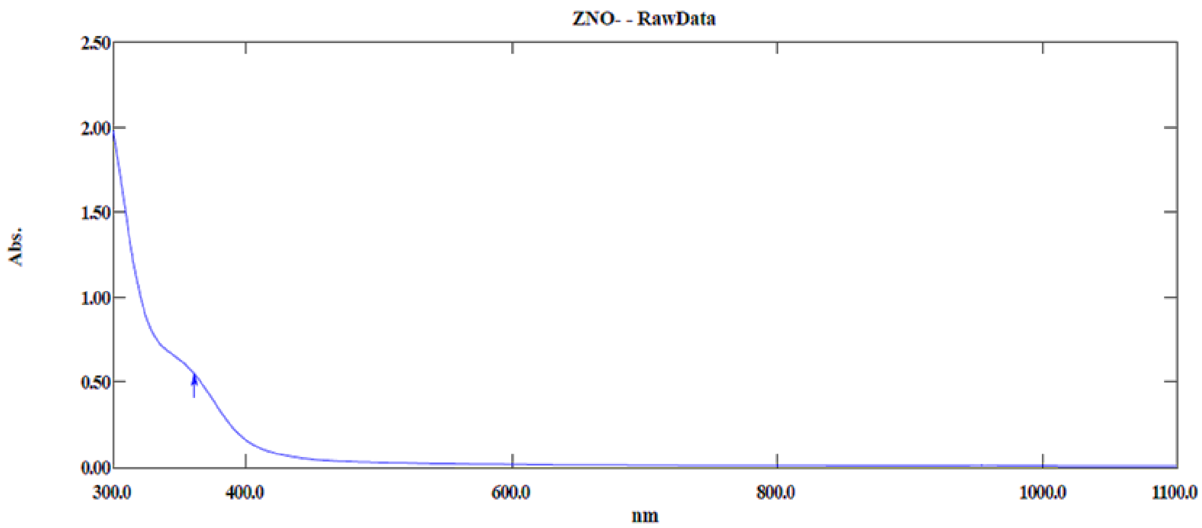

No.	Wavelength nm.	Absorbance	Description
1	361.0	0.546	

Figure 2. UV-Vis spectra of Photosynthesized Zinc Oxide Nanoparticles using Aas leaves extract (MC-ZnONPs).

The FTIR analysis for the Aas leaf extract and MC-ZnONPs shows in figure 3A, 3B and table1. The FTIR spectrum of Aas leaf extract showed vibration bands observed at 3545, 3474, 3248 2922, 1786, 1699, 1539, 1454, 1390, 1232, 1051 and 619, 524, 474, 416 cm^{-1} corresponds to O-H stretching, C-H asymmetric stretching, C-H symmetric stretching, bending vibrations of -OH, -C-O stretching, -C-O-C stretching and C-Cl stretching, respectively. The ZnO nanoparticles spectrum revealed vibration bands observed at 3421, 1764, 1633, 1037, 711, and 599, 453, 418 cm^{-1} due to the O-H stretching, C-H bending, and weak Zn-O stretching, respectively figure 3A. These functional groups are associated with the phyto-constituents of flavonoids, phenolics, tannin and phytic acid.

The ZnO nanoparticles spectrum revealed vibration bands observed at 3421, 711, and 599, 453 cm^{-1} due to the O-H stretching, C-H bending, and weak Zn-O stretching, respectively. At the same time, 573 cm^{-1} vibration band ascribed to the structure of ZnO figure3.

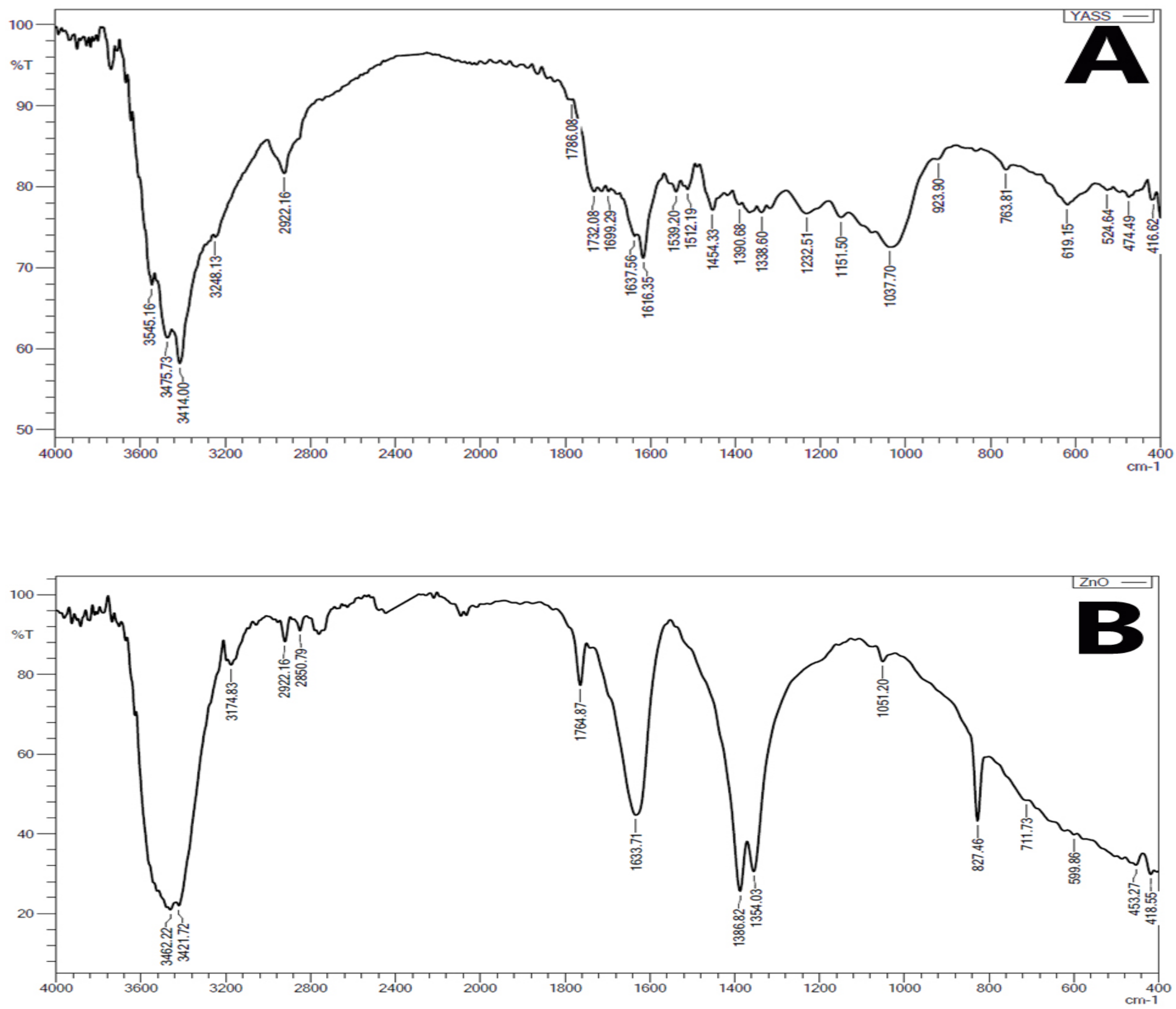

Figure 3. FT-IR spectra of Leaf extract of Aas, B- Photosynthesized Zinc Oxide Nanoparticles using Aas leaves extract (MC-ZnONPs).

Table1. Active groups present in the leaves extract of Aas which act as reducing, capping and stabilizing agent for Zinc Oxide Nanoparticles.

Peak No.	Absorption peak ()	Functional Group	Presence in plant Extract	Presence in ZnO-NPs	Interpretation
1	3545	O-H	Present	Disappeared	Reaction of hydroxyl and formation of new bonds on ZnO surface
2	3414, 3474	O-H	Present	Present/ Shifted to 3462, 3421	Reaction of hydroxyl with ZnO surface or increased particle size due to plant extract
3	3174, 3248	O-H	Present	Present/ Shifted	Reaction of hydroxyl with ZnO through adsorption or bonding
4	2922	C-H	Present	Absent/ Decreased	Indicates ZnO nanoparticle formation by plant extract
5	1732, 1764, 1786, 1699	C=O	Present	Present/ Shifted	Reaction of carbonyl group with surface or new bond formation (capping)
6	1616, 1633, 1637	C=C	Present	Present/Shifted	Reaction of aromatic group or amines with ZnO surface
7	1512, 1539	N-O	Present	Disappeared	Reaction with ZnO through bonding or stabilization
8	1454	C-H	Present	Disappeared	Reaction with ZnO surface
9	1386, 1338, 1390, 1354	O-H	Present	Present/Shifted	Reaction of hydroxyl with secondary metabolites formed
10	1232	C-N	Present	Disappeared/ Weakened	Confirmation of zinc reduction (Reduction) or capping
12	1037, 1151, 1051	C-O	Present	Disappeared/ Shifted to 1037–1051	Confirmation of ZnO nanoparticle formation through interaction with surface biomolecules
13	923	C=C	Present	Disappeared/ Weakened	Interaction with ZnO surface through ionic bonding
13	524, 619, 763, 711, 416, 474	C-H, C-Cl, C-Br, C-Zn, C-I	Present	Disappeared/ Shifted to 763–711	Appearance of new peak at 453 cm^{-1} with ZnO nanoparticle sample and another at 418 cm^{-1} confirming agreement with plant extract and vibrational bands of ZnO nanoparticles

X-ray diffraction is generally applied to a certain chemical arrangement and crystal design of an objective and it can be used for exposing the presence of ZnONPs. The specified crests are coordinated with the diffraction information of ZnO nanoparticles, the X-ray diffraction spectrum of photosynthesis zinc oxide nanoparticles corresponding to the main peaks obtained at 100, 001, 101, 102, 110, 103, 200, 112, 201, 004 and 202 correspond to reflections with 2θ values of the Bragg angles 32.19°, 34.84°, 36.67°, 47.94°, 56.98°, 63.24°, 66.74, 68.31°, 69.45, 72.92° and 76.58° respectively figure 3. These results confirm that the material tested are zinc oxide nanoparticles and are of high purity. In the meanwhile, the crystalline particles were calculated using the well-known Debye-Scherrer equation:

$D = [K\lambda/\beta\cos\theta]$ Å

Herein, the crystallite size is represented by the symbol (D), while K denotes the shape factor which is a constant (0.9) and λ is the x-ray wavelength (1.5406 Å).

The Bragg angle and corrected line broadening of the nanoparticles are represented by the symbols θ and β, respectively [26].

The average crystallite size according to Debye-Scherrer equation calculated was found to be 39.2 nm.

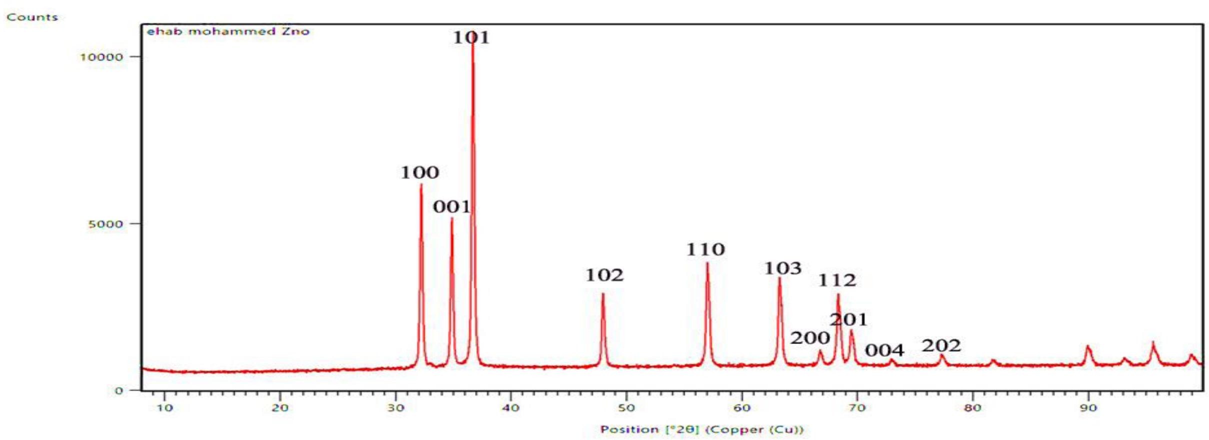

Figure 3. X-ray diffraction spectra of Photosynthesized Zinc Oxide Nanoparticles using Aas leaves extract (MC-ZnONPs).

Figure 4, shows a typical surface of prepared (MC-ZnONPs) from sodium selenite using Aas Leaves Extract reduction, the FESEM picture revealed a spherical in shape and aggregate into clusters. The size of these particles ranges from (21.86, 22.39, 27.85, 32.72, 37.75 and 43.94) nm.

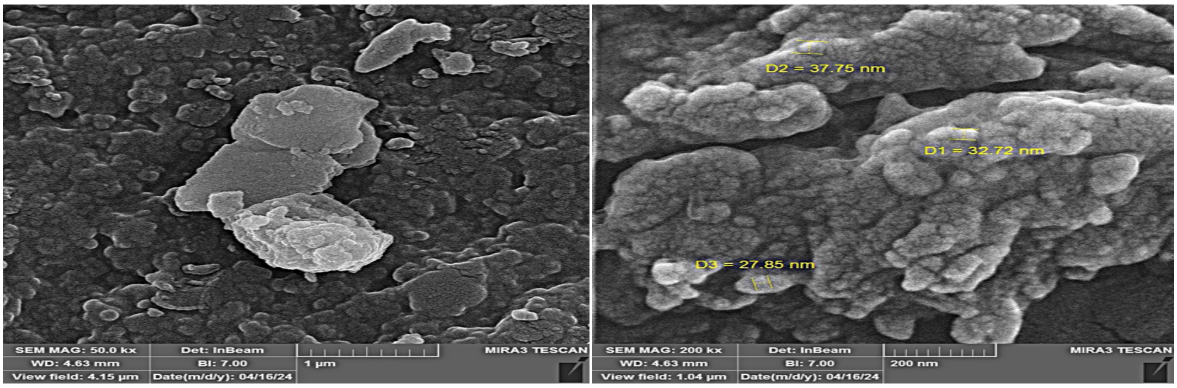

Figure 4. Field emission scanning electron microscopy image of Photosynthesized Zinc Oxide Nanoparticles using Aas leaves extract (MC-ZnONPs).

EDX elemental analysis of Photosynthesized Zinc Oxide nanoparticles using Aas Leaves extract exhibits the zinc signal along with carbon, oxygen, chlorine and copper; among these, the copper signal arises from the copper-coated grid; Sulfur and chlorine may be Some of these are attributed to the biogenic composition, while others are due to impurities. The EDX spectrum shown in figure 5, confirms the presence of an elemental form of Zinc Oxide.

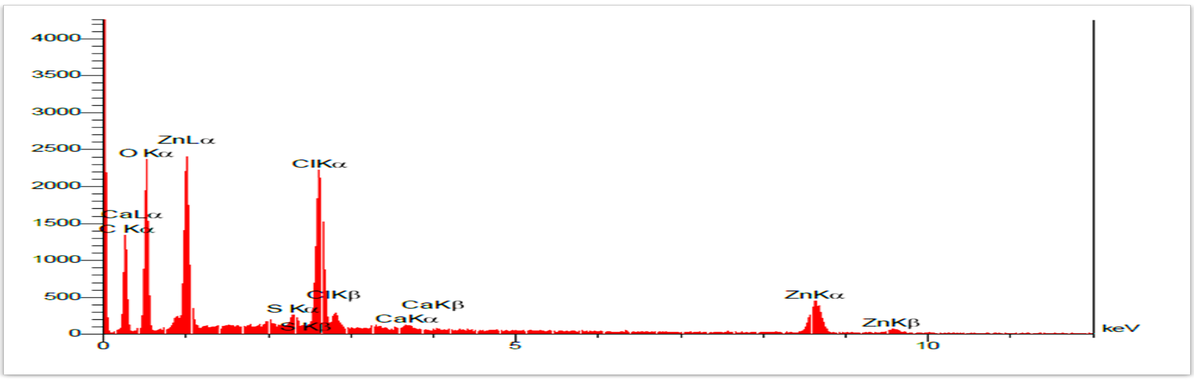

Figure 5. EDX elemental analysis of Photosynthesized Zinc Oxide nanoparticles using Aas Leaves extract (MC-ZnONPs).

Through atomic force microscopic analysis, the three-dimensional profile of the Photosynthesized Zinc Oxide nanoparticles using Aas Leaves Extract revealed the shape, porosity, surface topography, and height of the MC-ZnONPs. Figure 6 shows atomic force photomicrograph depicts the spherical-shaped nanoparticles distributed in a polydisperse manner, which also correlates with FE-SEM results. It is very clear from the 3D profile of MC-ZnONPs that the surface of the nanoparticle was smooth, and the average height of the nanoparticles was measured at 43 nm.

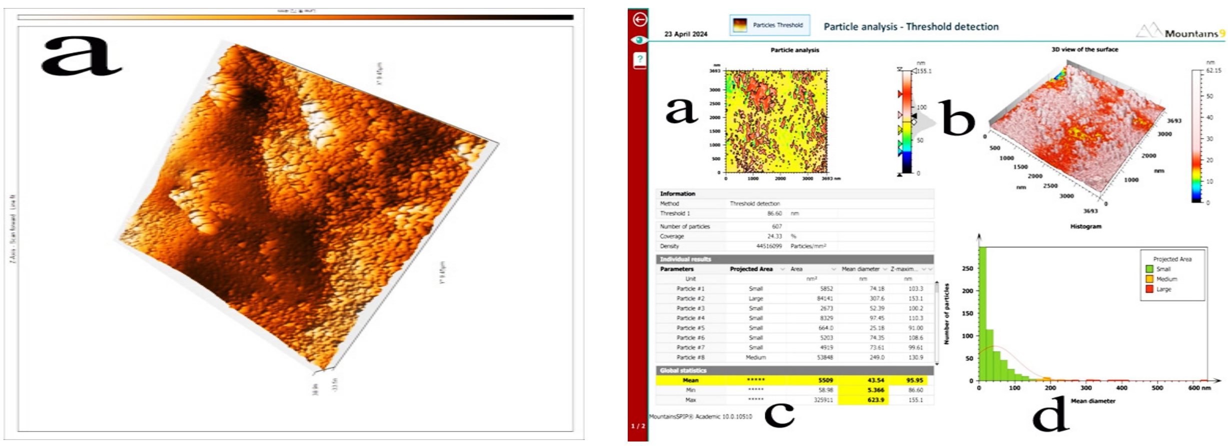

Figure 6. Atomic force imaging of (MC-ZnONPs). a, particles analysis, b, 3D view of surface, c, minimum and maximum of diameter and d, mean diameter.

The 2D image of the Photosynthesized Zinc Oxide nanoparticles using Aas Leaves Extract shows smaller individual particles of about 28.2 nm size, along with larger agglomerates of sizes up to ~150 nm while the 3D image indicates the presence of individual spherical particles, with maximum height of 38.9 nm in the z-direction.

Antimicrobial Activity of MC-ZnONPs by Resazurin (REMA)

The Antimicrobial Activity of ZnONPs on different *Acinetobacter baumannii* Isolates by Resazurin-based 96-well plate microdilution method showed that the minimum inhibitory concentration (MIC) of MC-ZnONPs was (156.25µg/ml), for *Acineto-*

bacter baumannii isolates number (2,3,4,5,6,7,8,9,10,16,17,18 and 20). The minimum inhibitory concentration (MIC) of MC-ZnONPs was (78.125µg/ml), for *Acinetobacter baumannii* isolates number (1,11,12,13,14,15 and 19). figure 7.

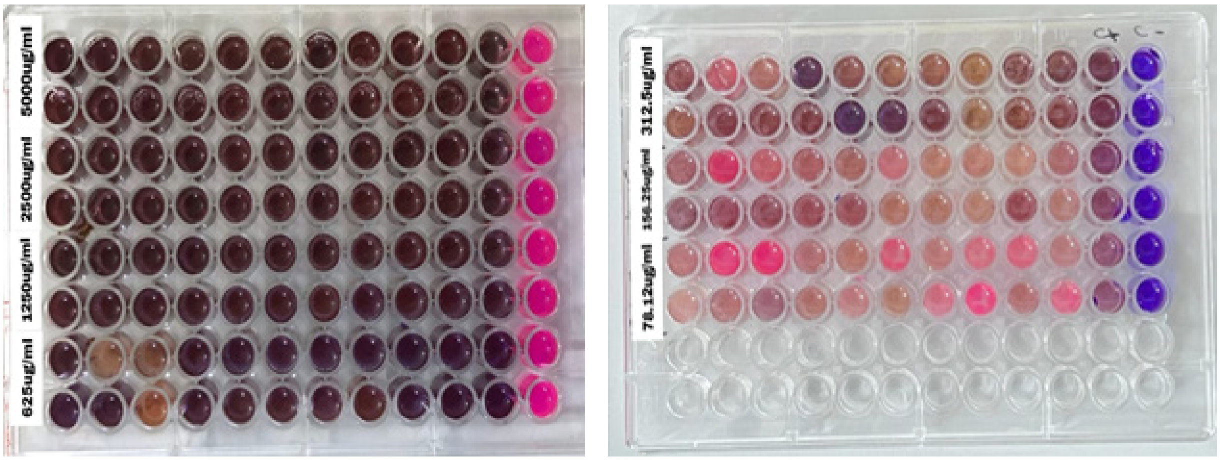

Figure 7. The MIC values of MC-ZnONPs on *A. baumannii* Isolates using REMA.

4. Discussion

Biological methods of synthesis nanomaterials are often preferred because they are clean, non-toxic, safe, biocompatible and environmentally acceptable. Zinc oxide nanoparticles are well-known to be one of the multifunctional inorganic compounds which are widely used in medical applications[27,28]. Zinc oxide nanoparticles are used as antimicrobial agent when incorporated into materials such as paints, textiles, plastics, cosmetics, a feed supplement in animal industry and personal care products. Aas (*Myrtus communis* L.) leaf extract was used in the present study for the photosynthesis of zinc oxide nanoparticles. Production of zinc oxide nanoparticles was confirmed by the formation of light yellow aggregates of zinc oxide nanoparticles. This result is in agreement with many studies [29,30] which found the formation of white aggregates is evidence of completeness of reaction and formation of zinc oxide nanoparticles. The produced crystalline zinc nanoparticles were confirmed by UV absorption spectrum at 370 nm this result is acceptance with several studies [31, 32] which reported that the peak absorption is at a range of 320-380 nm using UV-Visible spectroscope. The functional groups associated with the process of reducing and stabilizing zinc oxide nanoparticles were analyzed using Fourier Transform Infrared Spectroscopy. The results of FTIR analysis are in agreement with the finding of [33, 34].The results of AFM show the tip-corrected measured the size of ZnONPs in the range of 30-80 nm and showed the 3D view of the sample surface. These results are in agreement with several studies [35-36] in which found the variations in particle size distribution were found because of pH, the concentration of metal ion and incubation time. The results of X-ray diffraction spectrum of photosynthesis zinc oxide nanoparticles obtained the main reflections peaks at 100, 001, 101, 102, 110, 103, 200, 112, 201, 004 and 202 correspond to with 2θ values of the Bragg angles 31.70°, 34.34°, 36.16°, 47.54°, 56.48°, 62.78°, 66.23, 67.66°, 70.11, 72.53° and 76.58° respectively. These results are consistent with several studies in which biosynthesis of nanoparticles of zinc oxide molecules using plant extracts [37-38].

Produced zinc oxide nanoparticles were found to be irregular and polymorphic where the crystalline forms of these particles varied between rectangular, spherical, radial and cylindrical structures and the average size ranges between 28 - 43 nm using Scanning Electron Microscope theses finding are acceptance with many studies [39-40] in which found ZnONPs have different shapes and sizes depending on method conditions. The result of the present study shows that the Photosynthesized Zinc Oxide nanoparticles using Aas (*Myrtus communis* L.) leaves extract has effective antibacterial activities on the test isolates. These finding are in agreement with several studies [41, 42] in which they found ZnONPs synthesized by biological method has antibacterial activity against Gram positive and Gram negative bacteria. There are many mechanisms to kill bacteria by metallic nanoparticles such as cell wall damage and permeability, damage to nuclear material and protein synthesis, free radical release that cause reactive oxygen species (ROS) and other mechanics [43].

The results showed variation in the minimum inhibitory concentration (MIC) value of the synthesized ZnO nanoparticles depending on the bacterial isolates of *A. baumannii.* The current result is consistent with many local and foreign studies, including a study conducted in Iran by researchers [44], where the MIC concentration of biosynthesized ZnO nanoparticles that affected the gene expression of Adeb and AdeRS efflux pump genes for *A. baumannii* isolates ranged from 31.2-250 µg/ml. The results of the current study also agreed with the findings of a study conducted by [45], where the MIC concentration of biosynthesized ZnO nanoparticles against antibiotic-resistant *A. baumannii* isolates was 125 ug/ml. The current study also agreed with the results of [46], where her study was on the effect of zinc nanoparticles synthesized by Vitex agenus leaves against *P. aeruginosa* isolates, and the minimum inhibitory concentration was For ZnO it is 128 µg/ml, and in the study of [47], the minimum inhibitory concentration (MIC) of ZnO particles synthesized by *E. faecium* bacteria was 64 µg/ml and the sub-MIC was 32 µg/ml against *Proteus mirabilis* isolates and affected the gene expression of the motility gene *rsbA* in these bacteria.

5. Conclusions

We conclude from the present study the possibility of using the leaves extract of the Aas to prepare Zinc Oxide nanoparticles because the leaves of this plant are known for their rich content of flavonoids, alkaloids, tannins, terpenoids, and saponins, which appear to have the ability to reduce zinc salts and convert them into ZnO nanoparticles and also act as a capping and stabilizing agent.

Therefore, it can be concluded from the present study that Photosynthesized ZnO-NP can be developed as an alternative to antibiotics, that inhibit the growth of Multidrug resistant *A. baumannii* by producing ROS and causing membrane damage. Therefore, Photosynthesized ZnO nanoparticles can be more favorable future hope as an alternative drug to Multidrug resistant strain of *A. baumannii*.

Acknowledgments

Thanks and appreciation to Dr. Laith, Department of Biotechnology/ University of Baghdad, and Dr. Areej Alani, Department of Biology, College of Education for pure science Ibn al-Haytham, University of Baghdad. For their assistance in diagnosing the Aas plant and conducting tests on the properties of the nanomaterial.

References

1. J Jasem , A. and Maha A Mahmood 2025. Development and Characterization of Chitosan Nanoparticles Loaded with Amoxicillin as Advanced Drug Delivery Systems against Streptococcus Mutans. Ibn AL-Haitham Journal For Pure and Applied Sciences. 38, 1 (Apr. 2025), 1–15. DOI:https://doi.org/10.30526/38.1.3501

2. Johari B, Tavangar-Roosta S, Gharbavi M, Sharafi A, Kaboli S, Rezaeejam H. Suppress the cell growth of cancer stem-like cells (NTERA-2) using Sox2-Oct4 decoy oligodeoxynucleotide encapsulated niosomes-zinc hybrid nanocarriers under X irradiation. Heliyon. 2024;10(13). e34096. [PubMed ID: 39071677]. [PubMed Central ID: https://doi.org/10.1016/j.heliyon.2024.e34096. PMC11277410].

3. Saher T. Omar and Wand K. Ali. 2024. Effects of Zinc Oxide Nanoparticles (ZnO NPs) Synthesized from River Oak Casuarina cunninghamiana Miq.,1848 Leaf Extracts on Three Insects Species.). Iraqi Journal of Science, 65(12), 6946-6958. https://doi.org/10.24996/ijs.2024.65.12.12

4. Faiq, N.H. and Ahmed , M.E. 2024. Synergistic Inhibitory Effect of Biosynthesized ZnO-CuO Nanocomposite on Biofilm Formation of Proteus mirabilis. Ibn AL-Haitham Journal For Pure and Applied Sciences. 37, 2 (Apr. 2024), 49–63. DOI:https://doi.org/10.30526/37.2.3383.

5. Xue Y, bin Ismail AJ, Lansing MG, bin Mohd Hayati MF. Novel green synthesis of zinc oxide nanoparticles using Salvia rosmarinus extract for treatment of human lung cancer. Open Chem. 2023;21(1). https://doi.org/10.1515/chem-2023-0113.

6. Alhujaily M, Albukhaty S, Yusuf M, Mohammed MKA, Sulaiman GM, Al-Karagoly H, et al. Recent Advances in Plant-Mediated Zinc Oxide

Nanoparticles with Their Significant Biomedical Properties. Bioengineering (Basel). 2022;9(10). [PubMed ID: 36290509]. [PubMed Central ID: https://doi.org/10.3390/bioengineering9100541. PMC9598103].

7. Muhsen, Thamer & Hawar, Sumaiya & Mahdi, Tallal & Khaleel, Rihabi. (2020). Identification of CanEFFECT OF EUCALYPTUS AND MYRTUS EXTRACTS IDENTIFICATION BY GAS CHROMATOGRAPHY-MASS SPECTROMETRY ON SOME SPECIES OF CANDIDA AS A MODEL OF MEDICAL PLANTS candida species. Annals of Tropical Medicine and Public Health. 23. 10.36295/ASRO.2020.231032.

8. Grevsen K, Fretté XC, Christensen LP. Content and composition of volatile terpenes, flavonoids and phenolic acids in Greek oregano (Origanum vulgare L. ssp. hirtum) at different development stages during cultivation in cool temperate climate. Europ J Horticultural Sci. 2009;74(5):193-203. https://doi.org/10.1079/ejhs.2009/1182840.

9. Uysal Y, Gorkem Dogaroglu Z, Caylali Z, Karakulak DS. Rosemary Mediated Green Synthesis of ZnO Nanoparticles and their Integration into Hydrogel Matrices: Evaluating Effects on Wheat Growth and Antibacterial Properties. Glob Chall. 2024;8(11):2400120. [PubMed ID: 39545255]. [PubMed Central ID: PMC11557514]. https://doi.org/10.1002/gch2.202400120.

10. Al-Shmgani, Hanady & Mohammed, Hamdoon & Khalil, Khalil Abdullah. (2024). Synthesis and Characterization of Proteolytic Enzyme Loaded on Silver Nanoparticles. Ibn AL-Haitham Journal For Pure and Applied Sciences. 37. 10.30526/37.1.3300.

11. Keshavarz B, Gharbavi M, Bagherpour G, Rezaeejam H, Johari B. Green-Synthesized Silver Nanoparticles Coated with Alginate and Conjugated to Docetaxel Drug: Combination Therapy Under X Irradiation on LNCaP Prostate Cancer Cells. J Polymers Environ. 2025;33(7):3029-49. https://doi.org/10.1007/s10924-025-03591-8.

12. Kasem SM, Mahfouz ME, Mira NM, Helal IB. Evaluation of phytochemical profile, antioxidant activity, storage stability, in vitro release kinetics and cytotoxic effects of ultrasonicated Rosmarinus officinalis ethanolic

extract and its chitosan-loaded nanoparticles on chicken primary intestinal epithelial cells. Jokull J. 2023;73:29-68.

13. Shafey AME. Green synthesis of metal and metal oxide nanoparticles from plant leaf extracts and their applications: A review. Green Proces Synthesis. 2020;9(1):304-39. https://doi.org/10.1515/gps-2020-0031.

14. Adeyemi JO, Oriola AO, Onwudiwe DC, Oyedeji AO. Plant Extracts Mediated Metal-Based Nanoparticles: Synthesis and Biological Applications. Biomolecules. 2022;12(5). [PubMed ID: 35625555]. [PubMed Central https://doi.org/10.3390/biom12050627. ID: PMC9138950].

15. Agrawal, Pushpa; Mehta, Karan; Vashisth, Pooja; Sudarshan; Bhat, Preethi And Vishnu, B V Goutham. (2014). Green Synthesis Of Silver Nanoparticles And Their Application In Dental Filling Material. International Journal Of Innovative Research In Science, Engineering And Technology, Vol. 3, Issue 6.

16. Al-Abdeli, Intesar & Alkhalifawi, Isam. (2023). Antimicrobial and Antibiofilm Activity of Gold Nanoparticles Biosynthesized Using Acinetobacter Baumannii Isolated from Wounds and Burns. The Egyptian Journal of Hospital Medicine. 90. 1274-1283. 10.21608/ejhm.2023.282021.

17. Abdullah, Rana & Ahmed, Rasha & Al-Azzawi, Shahla. (2019). Genotyping of Acinetobacter baumannii by using BOX Method. Indian Journal of Forensic Medicine and Toxicology. 13. 934-938. 10.5958/0973-9130.2019.00418.3.

18. Manokari, M., Ravindran, C. P. and Shekhawat, M. S. (2016). Production of zinc oxide nanoparticles using aqueous extracts of amedicinal plant Micrococca mercurialis (L.) Benth. W.S.N., 30: 117-128.

19. Pillai, A.M., Sivasankarapillai, V.S., Rahdar, A., Joseph, J., Sadeghfar, F., Anuf A, R., Rajesh, K. and Kyzas, G.Z. 2020.Green synthesis and characterization of zinc oxide nanoparticles with antibacterial and antifungal activity. Journal of Molecular Structure, 1211, p.128107.

20. Supraja, S; Mohammed, Ali S ; Chakravarthy N ; Jayaprakash, Priya A ; Sagadevan E; Kasinathan M. K.; Sindhu S And Arumugam P. (2013). Green Synthesis of Silver Nanoparticles

From Cynodon Dactylon Leaf Extract. International Journal Of Chemtech Research, Vol.5,No.1, Pp: 271-277.

21. Gharbavi M, Johari B, Tabar RM, Sharafi A. Selenium doped albumin nanoparticles enhance tamoxifen induced anticancer effects in 4T 1 mouse breast cancer cells. Appl Organometallic Chem. 2023;38(2). https://doi.org/10.1002/aoc.7327.

22. Hassanpouraghdam MB, Mehrabani LV, Tzortzakis N. Foliar Application of Nano-zinc and Iron Affects Physiological Attributes of Rosmarinus officinalis and Quietens NaCl Salinity Depression. J Soil Sci Plant Nutrition. 2019;20(2):335-45. https://doi.org/10.1007/s42729 019-00111-1.

23. Alden, M. & Yaaqoob, Laith. (2022). EVALUATION OF THE BIOLOGICAL EFFECT SYNTHESIZED ZINC OXIDE NANOPARTICLES ON PSEUDOMONAS AERUGINOSA. IRAQI JOURNAL OF AGRICULTURAL SCIENCES. 53. 27-37. 10.36103/ijas.v53i1.1502.

24. Kaur H, Kumar S, Bouzid G. Exploring the role of different phytochemicals on the morphological variations of metal and metal oxide nanomaterials for biomedical application. Interactions. 2024;245(1). https://doi.org/10.1007/s10751-024-02088-5.

25. Ghaffarlou M, Rashidzadeh H, Mohammadi A, Mousazadeh N, Barsbay M, Sharafi A, et al. Photothermal and radiotherapy with alginate-coated gold nanoparticles for breast cancer treatment. Sci Rep. 2024;14(1):13299. [PubMed ID: 38858410]. [PubMed Central ID: PMC11164878]. https://doi.org/10.1038/s41598-024-60396-w.

26. Rashidzadeh H, Gharbavi M, Ghorbani R, Nazari M, Noei H, Johari B. Co Encapsulated Niosomes With Metformin and Silver Nanoparticles as Potential Anticancer Tool for the Combined Therapy on Lung Cancer Cells. Appl Organometallic Chem. 2025;39(7). https://doi.org/10.1002/aoc.70279.

27. Heidari S, Gharbavi M, Ghorbani R, Rezaeejam H, Johari B. Combined treatment using bismuth sulfide nanoparticles loaded with NANOG decoy oligodeoxynucleotides under X-ray radiation for breast cancer cells. Sci Rep. 2025;15(1):23131. [PubMed ID: 40594465]. [PubMed Central ID: PMC12219885]. https://

doi.org/10.1038/s41598-025-05074-1.

28. Al-Ghareebawi, A. M., Al-Okaily, B. N., & Ibrahim, O. M. S. (2021). CHARACTERIZATION OF ZINC OXIDE NANOPARTICLES SYNTHESIZED BY OLEA EUROPAEA LEAVES EXTRACT (PART L). IRAQI JOURNAL OF AGRICULTURAL SCIENCES, 52(3), 580-588. https://doi.org/10.36103/ijas.v52i3.1345

29. Aghapur N, Gharbavi M, Bigdelou Z, Zand M, Johari B. Green synthesis of silver nanoparticles coated with methotrexate-conjugated polyvinyl alcohol: As potential nanosystem for chemo/radiotherapy. J Drug Delivery Sci https://doi.org/10.1016/j.jddst.2025.106643. Technol. 2025;105.

30. Asadi N, Gharbavi M, Rezaeejam H, Farajollahi A, Johari B. Zinc nanoparticles coated with doxorubicin-conjugated alginate as a radiation sensitizer in triple-negative breast cancer cells. Int J Pharm. 2024;659:124285. [PubMed https://doi.org/10.1016/j.ijpharm.2024.124285. ID: 38821433].

31. Begum S, Kumuthini R. Characterization of zinc oxide nano particles synthesized via chemical and green method. Ovonic Res. 2023;19(5):505-12.

32. Saryanto H, Sebayang D. The simple fabrication of nanorods mass production for the dye-sensitized solar cell. MATEC Web of Conferences. EDP Sciences; 2017. 3006 p.

33. Alharbi FN, Abaker ZM, Makawi SZA. Phytochemical Substances—Mediated Synthesis of Zinc Oxide Nanoparticles (ZnO NPS). Inorganics. 2023;11(8). https://doi.org/10.3390/inorganics11080328.

34. Alprol AE, Eleryan A, Abouelwafa A, Gad AM, Hamad TM. Green synthesis of zinc oxide nanoparticles using Padina pavonica extract for efficient photocatalytic removal of methylene blue. Sci Rep. 2024;14(1):32160. [PubMed ID: 39741157]. [PubMed Central ID: PMC11688442]. https://doi.org/10.1038/s41598-024-80757-9.

35. Mohanasundaram P, Saral AM. Binding properties and biological applications of green synthesized ZnO nanoparticles from neem flower. Sci Rep. 2025;15(1):17727. [PubMed ID: 40399393]. [PubMed Central ID: PMC12095587]. https://doi.org/10.1038/s41598-025-02157-x.

36. . Faiq, Noor Hamza and Ahmed,

Mais E. (2024) “Effect of Biosynthesized Zinc oxide Nanoparticles on Phenotypic and Genotypic Biofilm Formation of Proteus mirabilis,” Baghdad Science Journal: Vol. 21: Iss. 3, Article 8.DOI: https://doi.org/10.21123/bsj.2023.8067

37. El-Belely EF, Farag MMS, Said HA, Amin AS, Azab E, Gobouri AA, et al. Green Synthesis of Zinc Oxide Nanoparticles (ZnO-NPs) Using Arthrospira platensis (Class: Cyanophyceae) and Evaluation of their Biomedical Activities. Nanomaterials (Basel). 2021;11(1). [PubMed ID: 33406606]. [PubMed Central https://doi.org/10.3390/nano11010095. ID: PMC7823323.

38. Elsehemy MS, Monam YK, Galhoum AA, Bayoumi EE, Gado WS, El Khair MA, et al. Synthesis, Characterization, and Evaluation of Zero Valent Iron Nanoparticles from Different Leaf Extracts: Photo Catalytic Dibenzothiophene Degradation and Antimicrobial Efficiency. Chem https://doi.org/10.1002/slct.202403785. Select. 2025;10(15).

39. Aldeen TS, Ahmed Mohamed HE, Maaza M. ZnO nanoparticles prepared via a green synthesis approach: Physical properties, photocatalytic and antibacterial activity. J Physics Chem Solids. 2022;160. https://doi.org/10.1016/j.jpcs.2021.110313.

40. Suleiman MH, El-Sheikh SM, Mohamed ET, El Raey MA, El Sherbiny S, Morsy FA, et al. Green synthesis of ZnO-NPs using sugarcane bagasse waste: phytochemical assessment of extract and biological study of nanoparticles. Dalton Trans. 2024;53(46):18494-505. [PubMed ID: 39474919]. https://doi.org/10.1039/d4dt02449d.

41.Saleh, F., Kheirandish, F., Hosseini, F., & Yazdian, F. (2021). Evaluation the effect of ZnO nanoparticle derived Bacillus subtilis on the expression of efflux pump genes (AdeB AdeRS) in Acinetobacter baumannii. Journal of environmental health science & engineering, 19(1), 1133–1141. https://doi.org/10.1007/s40201-021-00679.

42. Raha S, Ahmaruzzaman M. ZnO nanostructured materials and their potential applications: progress, challenges and perspectives. Nanoscale Adv. 2022;4(8):1868-925. [PubMed ID: 36133407]. [PubMed

Central ID: PMC9419838]. https://doi.org/10.1039/d1na00880c.

43. Abdelbaky AS, Abd El-Mageed TA, Babalghith AO, Selim S, Mohamed A. Green Synthesis and Characterization of ZnO Nanoparticles Using Pelargonium odoratissimum (L.) Aqueous Leaf Extract and Their Antioxidant, Antibacterial and Anti-inflammatory Activities. Antioxidants (Basel). 2022;11(8). [PubMed ID: 35892646]. [PubMed Central ID: PMC9329751]. https://doi.org/10.3390/antiox11081444.

44. Mohd Yusof H, Abdul Rahman N, Mohamad R, Zaidan UH, Samsudin AA. Biosynthesis of zinc oxide nanoparticles by cell-biomass and supernatant of Lactobacillus plantarum TA4 and its antibacterial and biocompatibility properties. Sci Rep. 2020;10(1):19996. [PubMed ID: 33204003]. [PubMed Central https://doi.org/10.1038/s41598-020-76402-w. ID: PMC7673015].

45.Supraja, S; Mohammed, Ali S ; Chakravarthy N ; Jayaprakash, Priya A ; Sagadevan E; Kasinathan M. K.; Sindhu S And Arumugam P. (2013). Green Synthesis of Silver Nanoparticles From Cynodon Dactylon Leaf Extract. International Journal Of Chemtech Research, Vol.5,No.1, Pp: 271-277.

46.Uysal Y, Gorkem Dogaroglu Z, Caylali Z, Karakulak DS. Rosemary Mediated Green Synthesis of ZnO Nanoparticles and their Integration into Hydrogel Matrices: Evaluating Effects on Wheat Growth and Antibacterial Properties. Glob Chall. 2024;8(11):2400120. [PubMed ID: 39545255]. [PubMed Central ID: PMC11557514]. https://doi.org/10.1002/gch2.202400120.

47.Xue Y, bin Ismail AJ, Lansing MG, bin Mohd Hayati MF. Novel green synthesis of zinc oxide nanoparticles using Salvia rosmarinus extract for treatment of human lung cancer. Open Chem. 2023;21(1). https://doi.org/10.1515/chem-2023-0113.